Decision-Feedback Frequency-Domain Volterra Nonlinear Equalizer for IM/DD OFDM Long-Reach PON

Junwei Zhang, Changjian Guo, Jie Liu, Xiong Wu, Alan Pak Tao Lau, Chao Lu and Siyuan Yu

***Abstract*—A low-complexity 3rd-order decision-feedback frequency-domain Volterra nonlinear equalizer (DF-FD-VNLE) with superior nonlinearity-compensation performance is proposed and experimentally demonstrated for OFDM long-reach PONs. High optical launch power up to 18 dBm is implemented to mitigate the chromatic dispersion (CD) induced power fading and increase the power budget. By reconstructing and subtracting the nonlinear noise in frequency domain with the knowledge of the nonlinear channel, the proposed DF-FD-VNLE outperforms the conventional time-domain VNLE (TD-VNLE) and feed-forward FD-VNLE (FF-FD-VNLE), resulting in better received signal-to-noise ratio (SNR) performance. The nonlinearity-compensation performance of the DF-FD-VNLE can be further improved with the usage of a FF-FD-VNLE or more than one iteration. Complexity and experimental analyses show that similar complexity and higher SNR can be achieved by using the one-iteration DF-FD-VNLE with FD linear equalization (FD-LE), compared with that of the FF-FD-VNLE. Compared with conventional TD-VNLE, the required number of real-valued multiplication (RNRM) of the one-iteration DF-FD-VNLE with FF-FD-VNLE (FD-LE) is reduced by a factor of as much as 82.19% (89.61%) at a memory length of 14 and a truncation factor of 3. Based on the one-iteration DF-FD-VNLE with FF-FD-VNLE, around 53.79 Gbit/s single wavelength OFDM IM-DD transmission over 60.8-km SSMF is successfully demonstrated at a BER of 3.8 × 10-3 and a received optical power (ROP) of -2 dBm, achieving 15% capacity improvement compared to the conventional TD-VNLE.**

***Index Terms*—Decision-feedback frequency-domain Volterra nonlinear equalizer (DF-FD-VNLE), intensity modulation and direct detection (IM-DD), orthogonal frequency division multiplexing (OFDM).**

Manuscript received December 14, 2018. This work is supported in part by National Natural Science Foundations of China (61505266, 61875233), Guangdong Natural Science Foundation (2016A030313289, 2018A0303130117), Local Innovative and Research Teams Project of Guangdong Pearl River Talents Program (2017BT01X121) and Pearl River S&T Nova Program of Guangzhou (201710010028). (*Junwei Zhang* and *Changjian Guo* contributed equally to this work.) (Corresponding authors: *Jie Liu* and *Changjian Guo*)

J. Zhang, J. Liu and X. Wu are with the State Key Laboratory of Optoelectronic Materials and Technologies, School of Electronics and Information Technology, Sun Yat-Sen University, Guangzhou 510006, China (e-mail: liujie47@mail.sysu.edu.cn).

C. Guo is with the South China Academy of Advanced Optoelectronics, South China Normal University, Guangzhou 510006, China and also with the Photonics Research Center, Department of Electronic and Information Engineering, The Hong Kong Polytechnic University, Hong Kong SAR, China (e-mail: changjian.guo@coer-scnu.org).

A. P. T. Lau is with the Photonics Research Center, Department of Electrical Engineering, The Hong Kong Polytechnic University, Hong Kong SAR, China.

C. Lu is the Photonics Research Center, Department of Electronic and Information Engineering, The Hong Kong Polytechnic University, Hong Kong SAR, China.

S. Yu is with the State Key Laboratory of Optoelectronic Materials and Technologies, School of Electronics and Information Technology, Sun Yat-Sen University, Guangzhou 510006, China and also with the Photonics Group, Merchant Venturers School of Engineering, University of Bristol, Bristol BS8 1UB, UK.

I. Introduction

Recently, development of high definition video and cloud computing etc., that using remote storage of data, has driven the demand for high-speed data transmission to the metro and access links [1], [2]. In order to increase the transmission capacity and meanwhile ensure low cost, long-reach passive optical networks (LR-PONs) with simplified architecture by consolidating the currently separate metro and access networks into an integrated network are recognized as one of the promising solutions for the next generation passive optical network 2 (NG-PON2) [3], [4]. Considering the high requirement of system cost and complexity of the LR-PONs, the intensity modulation and direct detection (IM-DD) schemes are preferred in practical implementations of the LR-PONs, although the coherent optical detection schemes often exhibit better performance [5]–[12]. Aiming at further increasing the system capacity by using currently mature and cost-effective 10 Gigabit-class devices, spectrally efficient modulations such as pulse-amplitude modulation (PAM), carrier-less amplitude phase modulation (CAP), and orthogonal frequency-division multiplexing (OFDM) have been received much attention in short reach optical transmission system [5]–[12]. Among them, OFDM has been considered as one of the good choices for downstream transmission in the NG-PON2, due to its flexible bandwidth allocation and high compatibility with time division multiplexing (TDM) and wavelength division multiplexing (WDM) techniques employed in XG-PON1 in addition to the high spectral efficiency [3], [4].

Nonetheless, chromatic dispersion (CD) induced power fading, nonlinear distortions and low loss budget are three main challenges to economical IM-DD OFDM LR-PONs [8]–[11]. CD induced power fading could be effectively mitigated by self-phase modulation (SPM) effect through launching high optical power to the fiber [8], [9]. In this situation, the system

power budget can be significantly improved, however, signal distortions resulting from fiber nonlinearity become much more severe, which will degrade the signal-to-noise ratio (SNR) performance of the IM-DD systems, similar with distortions due to nonlinear electro-optic modulation and square-law photo-detection. To compensate these nonlinear distortions, well-known time-domain Volterra nonlinear equalizer (TD-VNLE) has been extensively adopted in the IM-DD OFDM systems designed for LR-PONs [9]–[12]. However, the number of coefficients grows exponentially as the memory length increase for the conventional TD-VNLE [13], [14], which leads to high computational complexity and thus increase the cost and power consumption of the digital signal processing (DSP) module on the user side. In order to reduce the computational complexity, sparse TD-VNLE with much fewer coefficients using the orthogonal search approach has been proposed for IM-DD OFDM PON, which has achieved similar bit error ratio (BER) performance but lower complexity (28% taps reduction) compared to the conventional 3rd-order TD-VNLE [12]. A low complexity 3rd-order feed-forward frequency-domain VNLE (FF-FD-VNLE) has been proposed to compensate the nonlinear distortions at subcarrier level in IM-DD OFDM LR-PONs [10]. In addition to the computational complexity, the nonlinearity-compensation performance, which is related to the system capacity with bandwidth limited devices, should also be considered to be improved for the VNLE. As a result, consideration that is given to both of the nonlinearity-compensation performance and computational complexity of the VNLE is highly desired for the IM-DD OFDM LR-PONs.

In this paper, we propose a low complexity 3rd-order decision-feedback frequency-domain VNLE (DF-FD-VNLE) with superior nonlinearity-compensation performance for OFDM LR-PONs. We also apply high optical launch power up to 18 dBm to mitigate the CD induced power fading and increase the power budget. The proposed DF-FD-VNLE is aim to reconstructing and subtracting the nonlinear noise in frequency domain with the knowledge of the nonlinear channel, which exhibits a better received SNR performance, compared with that of the conventional TD-VNLE and feed-forward FD-VNLE (FF-FD-VNLE) presented in [10] under the same channel conditions. Moreover, the nonlinearity-compensation performance of the DF-FD-VNLE can be further improved with the usage of a FF-FD-VNLE or more than one iteration. Complexity and experimental analyses show that the required number of real-valued multiplication (RNRM) of the one-iteration DF-FD-VNLE with FD linear equalization (FD-LE) is similar to the FF-FD-VNLE, while the former obtains higher SNR. Compared with conventional TD-VNLE, the RNRM of the one-iteration DF-FD-VNLE with FF-FD-VNLE (FD-LE) is reduced by a factor of as much as 82.19% (89.61%) at a memory length of 14 and a truncation factor of 3. By utilizing the one-iteration DF-FD-VNLE with FF-FD-VNLE in an OFDM IM-DD transmission system over 60.8-km SSMF, the achievable capacity is around 53.79 Gbit/s at a BER of 3.8×10^{-3} and a received optical power (ROP) of -2 dBm, which is increased by a factor of around 15% compared with that of the conventional TD-VNLE.

The remainder of the paper is organized as follows. In section II, we describe the operating principle and computational complexity of the proposed DF-FD-VNLE. In section III, we discuss the experimental setup and results. Finally, Section VI summarizes and concludes this paper.

II. Operating Principle of the Proposed DF-FD-VNLE

A. The Simplified Frequency-Domain Volterra Series Nonlinear Channel Model

According to the analysis in [11], the whole IM-DD transmission channel with nonlinear impairments induced by electrical amplifiers, electro-optic modulators, fiber dispersion, fiber nonlinearity and photodiodes can be considered as a time-domain Volterra series model, in which the n^{th} sample of the received signal corrupted by the nonlinear distortions without considering the additive white Gaussian noise (AWGN) can be expressed as

$$r(n)=\sum_{k_1=0}^{N-1}h_1(k_1)x(n-k_1)+\sum_{k_1=0}^{N-1}\sum_{k_2=k_1}^{N-1}h_2(k_1,k_2)x(n-k_1)x(n-k_2)+\sum_{k_1=0}^{N-1}\sum_{k_2=k_1}^{N-1}\sum_{k_3=k_2}^{N-1}h_3(k_1,k_2,k_3)x(n-k_1)x(n-k_2)x(n-k_3)+\ldots \tag{1}$$

where $x(n-k_i)$ is the $(n\text{-}k_i)^{\text{th}}$ time sample of the transmitted signal, $h_b(k_1,k_2,\ldots k_b)$ is the coefficients of the b^{th}-order term of the nonlinear channel, and N is the memory length of the nonlinear channel. For time-domain Volterra series model in Eq. (1), the complexity of the b^{th}-order operation can be represented as $\frac{(N-1+b)!}{(b-1)!(N-1)!}$ [13]. Taking more high order terms into consideration may describe the nonlinear channel more accurately and lead to better performance in nonlinear equalization, but at the cost of increase of computational complexity and estimation instability in nonlinear compensation process due to the large number of coefficients [9]–[11]. To limit the complexity, terms higher than 3rd-order in Eq. (1) is neglected and only the diagonal multiplications with $k_1=k_2=k_3$ of 3rd-order operation are included, thus the complexity as well as the number of coefficients of the 3rd-order operation can be much reduced. Therefore, Eq. (1) is simplified as

$$r(n)=\sum_{k_1=0}^{N-1}h_1(k_1)x(n-k_1)+\sum_{k_1=0}^{N-1}\sum_{k_2=k_1}^{N-1}h_2(k_1,k_2)x(n-k_1)x(n-k_2)+\sum_{k_1=0}^{N-1}h_3(k_1)x^3(n-k_1) \tag{2}$$

By rearranging the 2nd-order term, we have

$$
\begin{aligned}
r(n) &= \sum_{k_1=0}^{N-1} h_1(k_1)x(n-k_1) \\
&+ \sum_{k_1=0,k_2=k_1}^{N-1} h_2(k_1,k_2)x(n-k_1)x(n-k_2) \\
&+ \sum_{k_1=0,k_2=k_1+1}^{N-1} h_2(k_1,k_2)x(n-k_1)x(n-k_2) \\
&+ \ldots + \sum_{k_1=0,k_2=k_1+N-1}^{N-1} h_2(k_1,k_2)x(n-k_1)x(n-k_2) \\
&+ \sum_{k_1=0}^{N-1} h_3(k_1)x^3(n-k_1)
\end{aligned} \tag{3}
$$

For the α^{th} term of 2nd-order operation in Eq. (3), $0 \le k_1 \le N-\alpha$ $(1 \le \alpha \le N)$ can be derived from $0 \le k_1 \le N-1$ and $k_2 = k_1 + \alpha - 1 \le N-1$. As a result, Eq. (3) can be rewritten as

$$
\begin{aligned}
r(n) &= \sum_{k_1=0}^{N-1} h_1(k_1)x(n-k_1) \\
&+ \sum_{k_1=0}^{N-1} h_2(k_1,k_1)x^2(n-k_1) \\
&+ \sum_{k_1=0}^{N-2} h_2(k_1,k_1+1)x(n-k_1)x(n-k_1-1) \\
&+ \ldots + \sum_{k_1=0}^{0} h_2(k_1,k_1+N-1)x(n-k_1)x(n-k_1-N+1) \\
&+ \sum_{k_1=0}^{N-1} h_3(k_1)x^3(n-k_1)
\end{aligned} \tag{4}
$$

By defining $x_{2,k}(n) = x(n)x(n-k)$, $h_{2,k}(n) = h_2(n, n+k)$ and $x_3(n) = x^3(n)$, Eq. (4) can be expressed as

$$
\begin{aligned}
r(n) &= h_1(n) * x(n) + h_{2,0}(n) * x_{2,0}(n) + h_{2,1}(n) * x_{2,1}(n) \\
&\quad + \ldots + h_{2,N-1}(n) * x_{2,N-1}(n) + h_3(n) * x_3(n) \\
&= h_1(n) * x(n) + \sum_{k=0}^{N-1} h_{2,k}(n) * x_{2,k}(n) + h_3(n) * x_3(n)
\end{aligned} \tag{5}
$$

where $*$ is the linear convolution operator. The 2nd-order nonlinear operation in Eq. (2) is divided into N parallel finite impulse response (FIR) linear filtering operations similar as the 1st-order linear operation. Since the value of $h_{2,k}(n)$ with a large k is expected to be very small [11], Eq. (5) can be simplified by retaining the first α linear convolution terms (i.e., the first α FIR filtering operations) of the 2nd-order operation to balance complexity and performance:

$$
r(n) = h_1(n) * x(n) + \sum_{k=0}^{\alpha-1} h_{2,k}(n) * x_{2,k}(n) + h_3(n) * x_3(n) \tag{6}
$$

where α is a truncation factor and also the number of FIR filters of 2nd-order operation. With the usage of cyclic prefix (CP) no less than the memory length N to avoid channel induced inter-symbol interference (ISI), linear convolution operator can be replaced with circular convolution operator after removing the CP. Thus the l^{th} time-domain sample ($l = 0, 1, 2, \cdots, M-1$, where M is the fast Fourier transform (FFT) size) of the p^{th} received OFDM symbol ($p = 0, 1, 2 \ldots \infty$) after removing the CP is

$$
r(l,p) = h_1(l) \otimes x(l,p) + \sum_{k=0}^{\alpha-1} h_{2,k}(l) \otimes x_{2,k}(l,p) + h_3(l) \otimes x_3(l,p) \tag{7}
$$

where $\otimes$ is the circular convolution operator, $x(l,p)$ is the l^{th} time-domain sample of the p^{th} transmitted OFDM symbol, $x_{2,k}(l,p) = x(l,p)x(< l-k >_M, p)$ and $x_3(l,p) = x^3(l,p)$, where $x(< l-k >_M, p)$ stands for k-point circular shift of $x(l,p)$. Then the simplified time-domain Volterra series model described in Eq. (7) can be transformed to simplified frequency-domain Volterra series model using M-point FFT

$$
\begin{aligned}
R(m,p) &= \sum_{l=0}^{M-1} r(l,p)e^{-j2\pi ml/M} \\
&= H_1(m)X(m,p) + \sum_{k=0}^{\alpha-1} H_{2,k}(m)X_{2,k}(m,p) \\
&\quad + H_3(m)X_3(m,p)
\end{aligned} \tag{8}
$$

where $X_b(m,p)$ (b = 1, 2, 3) and $R(m,p)$ are the M-point FFT outputs of $x_b(l,p)$ and $r(l,p)$, respectively. $H_b(m)$ is the b^{th}-order frequency-domain coefficients of the m^{th} subcarrier of the nonlinear channel.

B. The Proposed DF-FD-VNLE Based on the Simplified Frequency-Domain Volterra Series Nonlinear Channel Model

To equalize the nonlinear distortions of the received signal, conventional TD-VNLE can be performed at the receiver side. To limit the complexity, the n^{th} sample of the output signal after nonlinear equalization using conventional TD-VNLE with the same form as Eq. (2) is given by [9], [10]

$$
\begin{aligned}
y(n) &= \sum_{k_1=0}^{N_t-1} \omega_1(k_1)r(n-k_1) + \sum_{k_1=0}^{N_t-1} \sum_{k_2=k_1}^{N_t-1} \omega_2(k_1,k_2)r(n-k_1)r(n-k_2) \\
&\quad + \sum_{k_1=0}^{N_t-1} \omega_3(k_1)r^3(n-k_1)
\end{aligned} \tag{9}
$$

where $\omega_b(b = 1, 2, 3)$ is the coefficients of the b^{th}-order term of the conventional TD-VNLE, and N_t is the memory length of conventional TD-VNLE. The conventional TD-VNLE becomes the inverse of the nonlinear transmission channel only if the order of the nonlinear equalizer approaches the infinity [14], which is independent of the order of the nonlinear channel. Besides, the conventional TD-VNLE as a feed-forward equalizer suffers from noise enhancement in the present of AWGN compared to the decision-feedback equalizer [7]. In order to improve the nonlinearity-compensation performance, here we propose a 3rd-order DF-FD-VNLE by reconstructing and subtracting the nonlinear noise in frequency domain based on the simplified frequency-domain Volterra series nonlinear channel model. The output of the m^{th} subcarrier for the p^{th}

received OFDM symbol after subtracting the nonlinear terms using DF-FD-VNLE based on Eq. (8) can be expressed as

$$Y_{\text{DF-FD-VNLE}}(m,p) = \hat{H}_1^{-1}(m)[R(m,p) - \sum_{k=0}^{\alpha-1} \hat{H}_{2,k}(m)\tilde{X}_{2,k}(m,p) - \hat{H}_3(m)\tilde{X}_3(m,p)] \quad (10)$$

where $\tilde{X}_b(m,p)$ (b = 2, 3) is the estimated symbol of $X_b(m,p)$ obtained in frequency domain after symbol decision and OFDM modulation, and $\hat{H}_b(m)$ (b = 1, 2, 3) is the estimated value of $H_b(m)$. The nonlinear terms are reconstructed using $\tilde{X}_b(m,p)$ (b = 2, 3) and the estimated coefficients of the nonlinear channel. After subtracting the nonlinear terms, one-tap FD-LE is required to equalize the linear impairments. The estimated accuracy of $\tilde{X}_b(m,p)$ can be improved by iteration manner to further reduce the decision errors, thus improve the nonlinearity-compensation performance of DF-FD-VNLE.

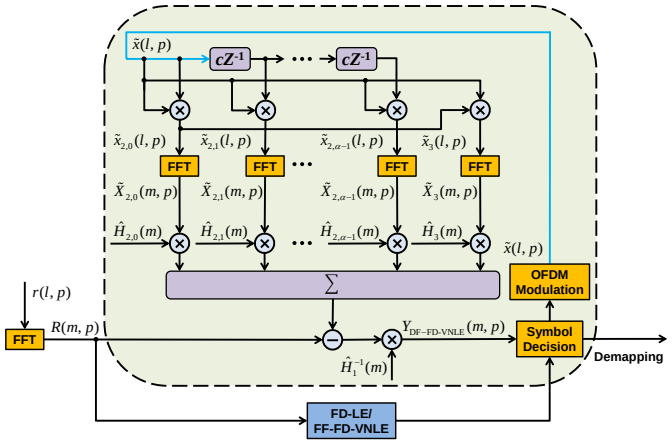

Fig. 1. Schematic diagrams of the proposed DF-FD-VNLE.

Fig. 1 shows the schematic diagram of the proposed DF-FD-VNLE. Here note that $l = 0, 1, 2, \cdots, M-1$ and $m = 0, 1, 2, \cdots, M-1$ represent M-point parallel time-domain and frequency-domain samples, respectively, and cZ^{-1} stands for unit circular shift. To reduce the decision errors and improve the reconstruction accuracy of the nonlinear terms, a FF-FD-VNLE presented in [10] instead of the FD-LE can be used before the first symbol decision. The FF-FD-VNLE is an inverse Volterra equalizer operating in frequency domain, which is the frequency-domain expression of the conventional TD-VNLE. The blue arrow represents the output of the reconstructed time-domain transmitted signal, which is then processed to obtain the $\tilde{X}_b(m,p)$ (b = 2, 3). After reconstructing the nonlinear terms, the signal can be equalized using DF-FD-VNLE by eliminating the nonlinear noise of the received signal. The coefficients of the nonlinear channel are obtained by utilizing a certain length of training symbols at the beginning of the data transmission according to the least squares (LS) algorithm [15]. Here it should be noted that least mean squares (LMS) estimation or recursive least squares (RLS) algorithm [15] can also be employed here for higher accuracy or faster convergence. The procedures of nonlinear coefficients estimation using P training symbols of the DF-FD-VNLE are summarized as:

We define the three following vectors and matrixes refer to Eq. (8):

1) The frequency-domain received training symbol vector:

$$\mathbf{R}_P = [R(m,0), R(m,1), \cdots, R(m,P-1)]^T \quad (11)$$

where $(\bullet)^T$ stands for transposition.

2) The frequency-domain transmitted training symbol matrix:

$$\mathbf{X}_P = \begin{bmatrix} X(m,0) & X(m,1) & \cdots & X(m,P-1) \\ X_{2,0}(m,0) & X_{2,0}(m,1) & \cdots & X_{2,0}(m,P-1) \\ X_{2,1}(m,0) & X_{2,1}(m,1) & \cdots & X_{2,1}(m,P-1) \\ \vdots & \vdots & \ddots & \vdots \\ X_{2,\alpha-1}(m,0) & X_{2,\alpha-1}(m,1) & \cdots & X_{2,\alpha-1}(m,P-1) \\ X_3(m,0) & X_3(m,1) & \cdots & X_3(m,P-1) \end{bmatrix}^T \quad (12)$$

3) The frequency-domain nonlinear channel vector:

$$\mathbf{H} = [H_1(m), H_{2,0}(m), H_{2,1}(m), \cdots, H_{2,\alpha-1}(m), H_3(m)]^T \quad (13)$$

After that, the following relationship of Eq. (8) considering AWGN can be obtained:

$$\mathbf{R}_P = \mathbf{X}_P\mathbf{H} + \mathbf{Z} \quad (14)$$

where $\mathbf{Z}$ is the frequency domain AWGN matrix with zero mean and a variance σ^2. Then the LS estimation can be performed to obtain the frequency-domain nonlinear channel:

$$\hat{\mathbf{H}} = (\mathbf{X}_P^H\mathbf{X}_P)^{-1}\mathbf{X}_P^H\mathbf{R}_P \quad (15)$$

where $(\bullet)^H$ stands for conjugate transposition.

C. Complexity Analysis

TABLE I. COMPLEXITY ANALYSIS OF THE FD-LE, CONVENTIONAL TD-VNLE, FF-FD-VNLE AND ONE-ITERATION DF-FD-VNLE IN ONE OFDM SYMBOL.

Method	Operation Category	Size of Operation	Number of Operation	RNRM
FD-LE	TD	0	0	0
	FFT	$M(\log_2 M-3)/2+2$	1	$M(\log_2 M-3)/2+2$
	FD	3	S	$3S$
Conventional TD-VNLE [13]	TD	$N_t^2+5N_t$	M	$M(N_t^2+5N_t)$
	FFT	$M(\log_2 M-3)/2+2$	1	$M(\log_2 M-3)/2+2$
	FD	0	0	0
FF-FD-VNLE [10]	TD	M	$(\alpha+1)$	$M(\alpha+1)$
	FFT	$M(\log_2 M-3)/2+2$	$(\alpha+2)$	$[M(\log_2 M-3)/2+2](\alpha+2)$
	FD	$3(\alpha+2)$	S	$3S(\alpha+2)$
One-iteration DF-FD-VNLE	TD	M	$(\alpha+1)$	$M(\alpha+1)$
	FFT	$M(\log_2 M-3)/2+2$	$(\alpha+1)$	$[M(\log_2 M-3)/2+2](\alpha+1)$
	IFFT	$M(\log_2 M-3)/2+2$	1	$M(\log_2 M-3)/2+2$
	FD	$3(\alpha+2)$	S	$3S(\alpha+2)$

The total complexity (TD operation + FFT/inverse FFT (IFFT) + FD operation) of the proposed DF-FD-VNLE in one OFDM symbol based on Eq. (10) in terms of the RNRM is analyzed and compared with conventional TD-VNLE and

FF-FD-VNLE as shown in Table I. M and S are the FFT size and the number of data-carrying subcarriers, respectively. For conventional TD-VNLE in Eq. (9), the total number of 1st-, 2nd- and 3rd-order nonlinear coefficients are N_t, $N_t(N_t+1)/2$ and N_t, respectively. With respect to complexity, N_t, $N_t(N_t+1)$ and $3N_t$ real-valued multiplications are required to perform each sample output for 1st-, 2nd- and 3rd-order operations in Eq. (9), respectively [13]. After performing conventional TD-VNLE in time domain, the equalized signal is needed to be transformed to frequency domain for demodulation with one real-valued FFT operation. For DF-FD-VNLE in Eq. (10), the total number of nonlinear coefficients is $(\alpha+2)S$. In each iteration, $\alpha+1$ real-valued FFT operations are required to convert the delay-multiply signals to frequency domain after the symbol decision and OFDM modulation, as clearly shown in Fig. 1. One IFFT process is also required in real-valued OFDM modulation. Since the signal is equalized in frequency domain, $\alpha+2$ complex-valued multiplications are needed for each data-carrying subcarrier. Here we choose real-valued split-radix FFT algorithm for FFT operation, in which $M(\log_2 M-3)/2+2$ real-value multiplication is required to execute M-point real-valued FFT [16]. Here note that the FFT output of a real-value sequence has complex conjugate symmetry. The complex-valued IFFT for M-point complex conjugate symmetric sequence is the inverse process of real-value FFT and thus the same RNRM with it, as shown in Table I. In addition, each complex multiplication is performed with 3 real-valued multiplications [16]. The complexity of the FF-FD-VNLE [10] with the same RNRM as the one-iteration DF-FD-VNLE is also included in Table I.

By taking the advantage of efficient FFT algorithm and avoiding linear convolution operator, the proposed DF-FD-VNLE as well as FF-FD-VNLE have lower algorithm complexities than the conventional TD-VNLE method. Figs. 2(a) and 2(b) present the specific RNRM versus the memory length in one OFDM symbol for the conventional TD-VNLE, compared with that of the FF-FD-VNLE and DF-FD-VNLE at a truncation factor of 3 and a truncation factor of 1, respectively. The conventional TD-VNLE with diagonal truncation represents that only the diagonal multiplications with $k_1 = k_2$ of 2nd-oder operation are included. M = 1024 and S = 170 are used here as well as in the experiments. Note that the number inside bracket in the figure caption denotes the number of iterations. It can be seen that the RNRM of the one-iteration DF-FD-VNLE with FD-LE is similar to the FF-FD-VNLE, which is much lower than that of conventional TD-VNLE. Besides, the RNRMs of the FD-VNLEs only depend on the FFT size instead of the memory length, providing that a CP with sufficient number of samples is used to ensure the circularity of the nonlinear channel in Eq. (7). Figs. 2(c) and 2(d) show the RNRM reductions of FD-VNLE schemes over conventional TD-VNLE at a truncation factor of 3 and a truncation factor of 1, respectively. Compared with conventional TD-VNLE, 82.19% and 89.61% of RNRMs can be saved by using one-iteration DF-FD-VNLE with FF-FD-VNLE and one-iteration DF-FD-VNLE with FD-LE, respectively, at a memory length of 14 and a truncation factor of 3. In the case of performing diagonal truncation of 2nd-order operation for all equalizers, the complexity savings reduced to 68% and 79.43% for one-iteration DF-FD-VNLE with FF-FD-VNLE and FD-LE, respectively.

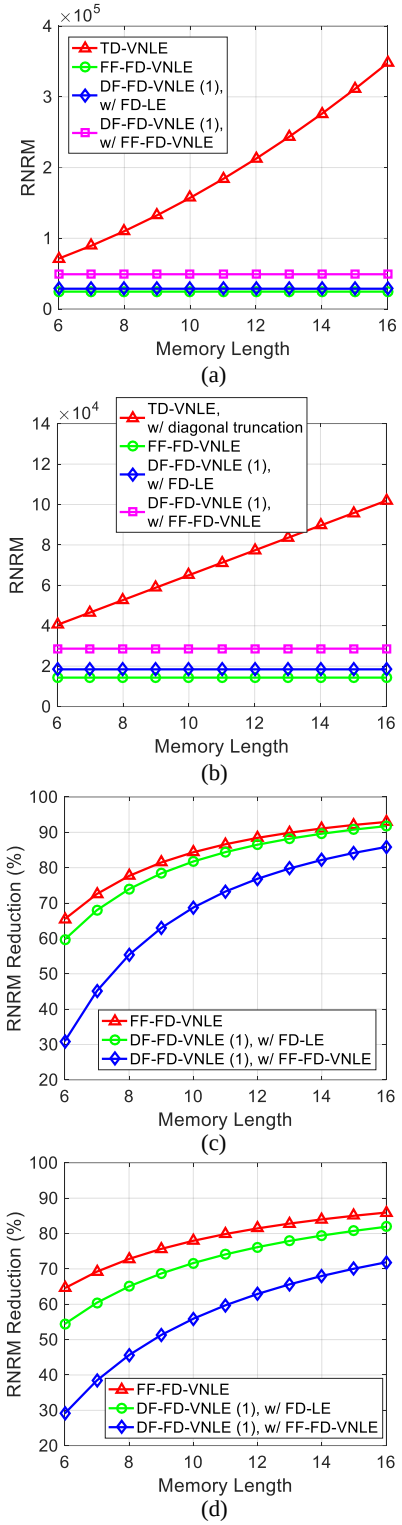

Fig. 2 (a) RNRMs of the conventional TD-VNLE at different memory length, FF-FD-VNLE and one-iteration DF-FD-VNLE at a truncation factor of 3; (b) RNRMs of the conventional TD-VNLE with diagonal truncation at different memory length, FF-FD-VNLE and one-iteration DF-FD-VNLE at a truncation factor of 1; (b) RNRM reductions of FF-FD-VNLE and one-iteration DF-FD-VNLE at (c) a truncation factor of 3 over conventional TD-VNLE and (d) a truncation factor of 1 over conventional TD-VNLE with diagonal truncation.

III. Experimental Setup and Results

A. System Setup

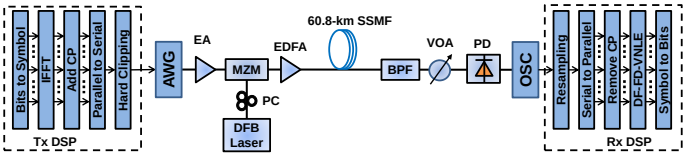

Fig. 3 Experimental setup and DSP block diagram. AWG: arbitrary waveform generator; EA: electrical amplifier; MZM: Mach-Zehnder modulator; DFB: distributed feedback; PC: polarization controller; EDFA: erbium doped fiber amplifier; SSMF: standard single mode fiber; BPF: band-pass filter; VOA: variable optical attenuator; PD: photo detector; OSC: real time oscilloscope.

Table II. Frame structures for experiment.

Items	Value
FFT size	1024
Modulated subcarriers	170
CP size	22
Modulation formats	Adaptive bit loading using *m*-QAM
Signals used	OFDM
Symbols per frame	500
Training symbols per frame	50 for BER measurement
	10 - 200 for SNR measurement
Data symbols per frame	450 for BER measurement
	300 - 490 for SNR measurement

Fig. 3 illustrates the experimental setup of the OFDM transmission system based on the proposed DF-FD-VNLE. At the transmitter, the frequency-domain quadrature amplitude modulation (QAM) symbols after adaptive bit and power loading [17] are converted to time domain by 1024-point IFFT. The effective payload and their complex conjugates are encoded at the 2nd to 171st and 1024th to 855th subcarriers, respectively. After adding 22-point CP, parallel-to-serial (P/S) conversion and hard clipping, the signal is then loaded into an arbitrary waveform generator (AWG) operating at a sample rate of 60 GSa/s to generate the electrical signal with a bandwidth of around 10 GHz. The frame structures are clearly shown in Table II. For each transmission, total 500 symbols including the training symbols with binary phase shift keying (BPSK) format and the effective data symbols are transmitted. The total number of transmitted symbols is limited by the output length of the AWG. Then the electrical OFDM signal is amplified by an electrical amplifier (EA) and utilized to drive a Mach-Zehnder modulator (MZM). The optical carrier with a wavelength of 1550.12 nm is generated by a distributed feedback (DFB) laser, followed by a polarization controller (PC) used to align the state of polarization (SOP) of the optical carrier with the MZM. The generated optical signal is amplified by an erbium doped fiber amplifier (EDFA) to enable the optical launch power up to 18 dBm. Here note that coherence control by low-speed frequency modulation (FM) of the DFB laser is enabled to reduce the unwanted stimulated Brillouin scattering (SBS) effect resulting from the strong optical launched power [8]. After 60.8-km SSMF transmission without any optical amplification, the optical signal is detected by an optical receiver consisting of an optical band-pass filter (BPF), a variable optical attenuator (VOA) and a photo detector (PD). The detected signal is then digitized and stored by a real time oscilloscope (OSC) operating at a sampling rate of 100 GSa/s. This is followed by an off-line DSP including resampling to 60 GSa/s to ensure 1 sample per symbol for FFT, timing synchronization, serial-to-parallel (S/P) conversion, DF-FD-VNLE, demodulation and bit error counting.

B. Experimental Results and Discussion

We first optimize the memory length for the conventional TD-VNLE and the truncation factor for the DF-FD-VNLE and FF-FD-VNLE at a ROP of -2 dBm after 60.8-km SSMF transmission. We perform channel estimation with 200 BPSK training symbols, following 300 16-QAM symbols for SNR measurement. Fig. 4(a) shows the average SNR versus the memory length for the conventional TD-VNLE. One can see that the SNR performance after using the conventional TD-VNLE is improved as the memory length increases until it reaches saturation when the memory length is no less than 14. About 0.9-dB average SNR degradation can be observed for the conventional TD-VNLE after diagonal truncation for the 2nd-order operation. Fig. 4(b) presents the average SNR versus the truncation factor for the DF-FD-VNLE and FF-FD-VNLE. The FD-LE or FF-FD-VNLE is performed before the symbol decision for the DF-FD-VNLE. The DF-FD-VNLE without decision errors achieving the best performance is also implemented for comparison, in which the nonlinear noise is virtually eliminated by substituting the transmitted signal X for $\tilde{X}$ in Eq. (10). It can be seen that: 1) The SNR performance of DF-FD-VNLE and FF-FD-VNLE are saturated at a truncation factor of no less than 3. 2) The average SNR of the one-iteration DF-FD-VNLE with FD-LE is better than that of the conventional TD-VNLE and FF-FD-VNLE due to the fact that the conventional TD-VNLE suffers from noise enhancement in the present of AWGN, which can be mitigated by the symbol decision [7]. 3) Due to the reduction of the decision errors, the average SNR of the DF-FD-VNLE can be further improved with FF-FD-VNLE instead of FD-LE or more iterations, which is close to that of the DF-FD-VNLE without decision errors. To balance the performance and complexity, a truncation factor of 3 and a memory length of 14 are set for the DF-FD-VNLE and conventional TD-VNLE in the following experiments, respectively. In addition, the FF-FD-VNLE is performed before the symbol decision to improve the equalization performance and only one iteration is constrained for the DF-FD-VNLE. For concision, the results of FF-FD-NE with similar performance as conventional TD-VNLE are omitted in the following experiments.

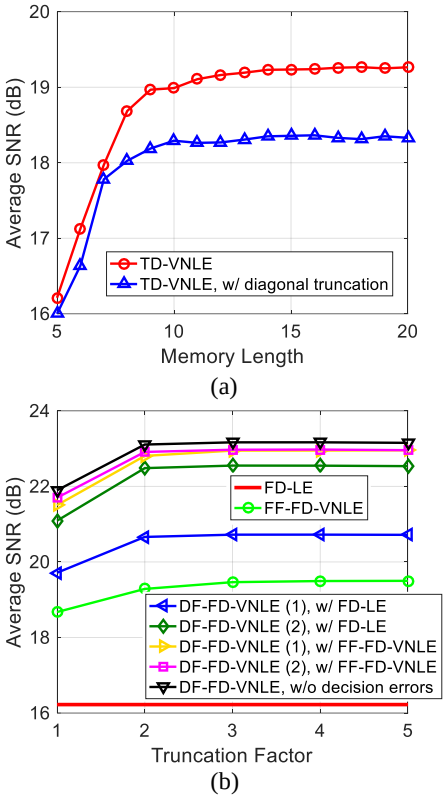

Fig. 4 (a) Average SNR versus the memory length for the conventional TD-VNLE and (b) the truncation factor for the DF-FD-VNLE and FF-FD-VNLE. The SNR values are measured at a ROP of -2 dBm after 60.8-km SSMF transmission.

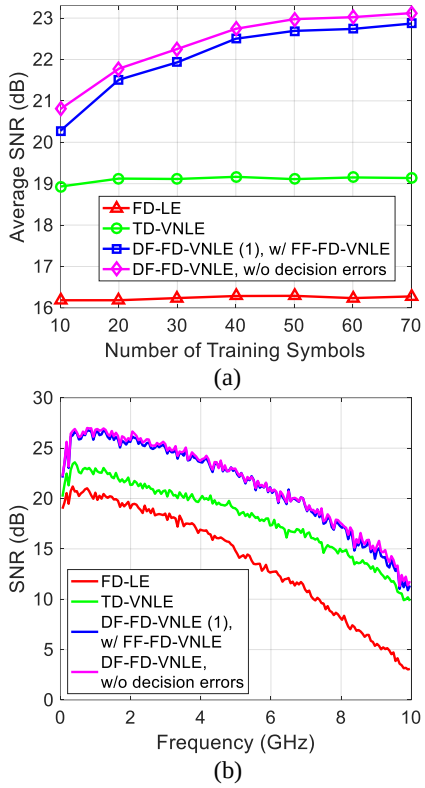

Fig. 5 (a) Average SNR versus the number of training symbols for the FD-LE, conventional TD-VNLE and DF-FD-VNLE; (b) Measured SNR curves within the signal bandwidth. The SNR values are measured at a ROP of -2 dBm after 60.8-km SSMF transmission.

The dependence of the average SNR performance on the length of training symbols for the FD-LE, conventional TD-VNLE and DF-FD-VNLE are shown in Fig. 5(a). It can be seen that the DF-FD-VNLE achieves the best average SNR performance, which is more than 3 dB (6 dB) higher than that of the conventional TD-VNLE (FD-LE) when the number of training symbols is no less than 40. The DF-FD-VNLE need more training symbols to achieve the optimal performance compared with conventional TD-VNLE, due to the fact that the number of coefficients in DF-FD-VNLE is much more than that in conventional TD-VNLE. To limit the training overhead, 50 training symbols and 450 effective data symbols are set for BER test, which results in 10% training overhead. It is noted that the training overhead can be reduced by increasing the number of effective data symbols or employing efficient channel estimation method such as intra-symbol frequency-domain averaging (ISFA) in frequency domain [18]. The measured SNR curves within the signal bandwidth are also depicted in Fig. 5(b), showing that the SNR improvement of DF-FD-VNLE is much better than that of the conventional TD-VNLE.

To show the advantage of the SPM effect with high optical launch power, the electrical spectra and SNR results at a ROP of -8 dBm after 60.8-km SSMF transmission are shown in Fig. 6, with 9-dBm and 18-dBm optical launch power. One can see that: 1) when the optical launch power is set to 9-dBm, a deep fading at around 8.5GHz can be observed, while the fading is effectively mitigated when an 18-dBm launch power is used. This is due to the negative phase shift introduced by the SPM effect, which cancelled the CD induced phase shift. As a result, the power budget and transmission bandwidth are also significantly increased. 2) Due to the reduced transmission nonlinearity at 9-dBm optical launch power compared with the 18-dBm launch power cases, the SNR improvements of all nonlinear equalization schemes are also less significant, as shown in Figs. 6(b) and 6(c), especially in high frequency range. 3) TD-VNLE is not effective at 9-dBm launch power, even when the memory length is increased to 20. In contrast, for DF-FD-VNLE, hard decision is performed before calculating the nonlinear noise, thereby avoiding the noise enhancement effect and leading to a better SNR.

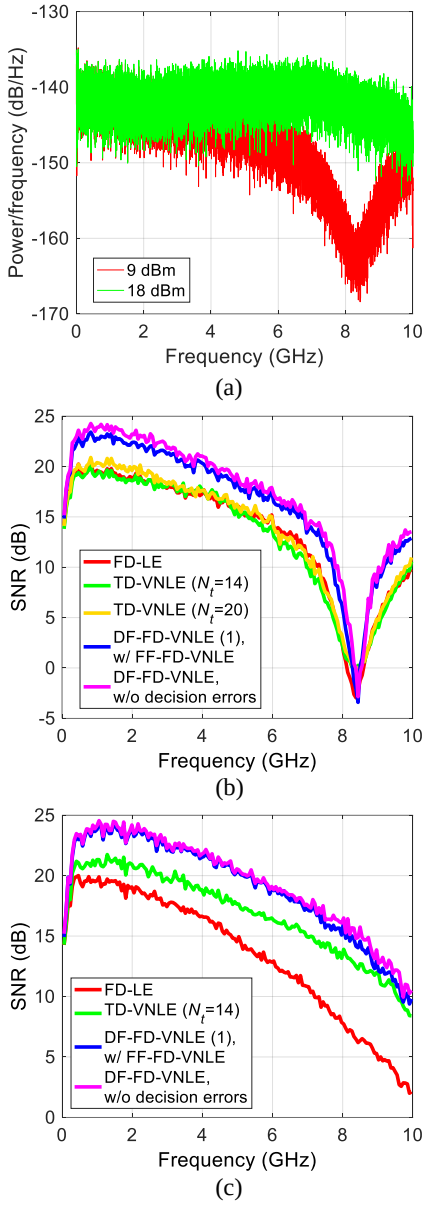

Fig. 6 (a) Measured electrical spectra and SNR curves within the signal bandwidth with (b) 9-dBm and (c) 18-dBm optical launch power at a ROP of -8 dBm after 60.8-km SSMF transmission.

By taking advantage of the SNR improvement with effective nonlinear equalization, the capacity of the transmission system can be further improved. The measured BER versus data rate using different equalization methods at a ROP of -2 dBm over 60.8-km SSMF transmission is shown in Fig. 7(a). Due to existing residual nonlinearity resulting from decision errors, the achieved data-rate of the one-iteration DF-FD-VNLE with FF-FD-NE is lower than that of the DF-FD-VNLE without decision errors case. The achievable capacity of the one-iteration DF-FD-VNLE with FF-FD-NE is around 53.79 Gbit/s at a BER of 3.8 $\times 10^{-3}$, which is increased by a factor of around 15% compared with 46.82-Gbit/s data rate of conventional TD-VNLE. Taking all of overhead into account (i.e., CP, training symbols and hard-decision forward error correction (HD-FEC)), the net data rate is 53.79 $\times$ 1024/(1024+22) $\times$450/500 $\times$(1-7%) = 44.08 Gbit/s at a ROP of -2 dBm, achieving an effective spectral efficiency of 4.41 bit/s/Hz. Moreover, the corresponding bit and power loading profiles and received constellations of 5-bit carrying subcarriers for the FD-LE, conventional TD-VNLE and one-iteration DF-FD-VNLE with FF-FD-NE at a data rate of 53.79 Gbit/s are shown in Figs. 7(b)–7(d) and Figs. 7(e)–7(g), respectively.

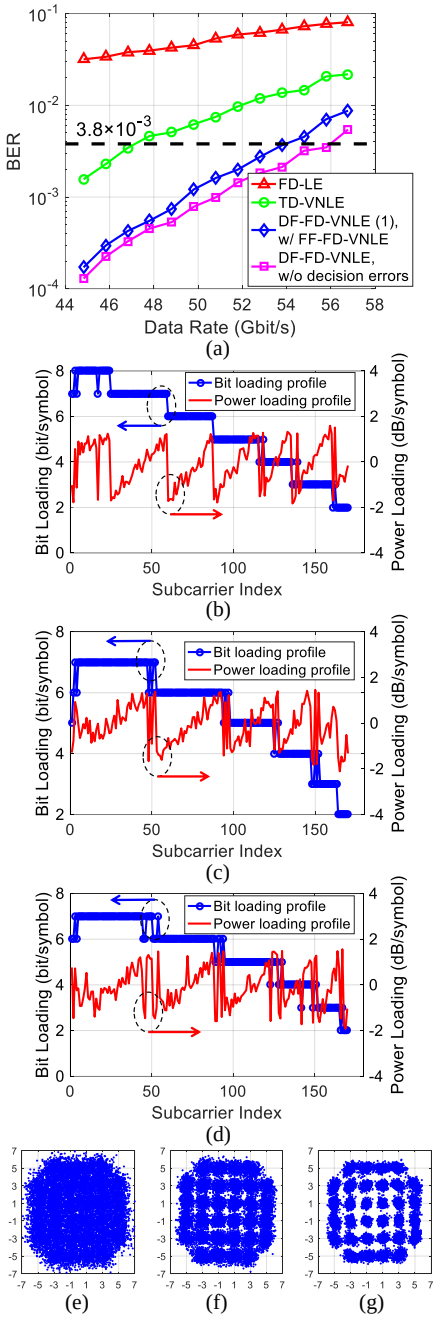

Fig. 7 (a) Measured BER versus date rate at a ROP of -2 dBm over 60.8-km SSMF transmission by utilizing adaptive bit and power loading; The corresponding bit and power loading profiles for the (b) FD-LE, (c) conventional TD-VNLE and (d) one-iteration DF-FD-VNLE with FF-FD-NE at a data rate of 53.79 Gbit/s; The received constellations of 5-bit carrying subcarriers for the (e) FD-LE, (f) conventional TD-VNLE and (g) one-iteration DF-FD-VNLE with FF-FD-NE at a data rate of 53.79 Gbit/s.

IV. Conclusions

In this paper, we have proposed and experimentally demonstrated a DF-FD-VNLE with superior nonlinearity-compensation performance for OFDM LR-PONs. Both theoretical analysis and experimental measurement have been carried out to verify the feasibility and advantage of the proposed DF-FD-VNLE. The results of complexity analysis and experiment showed that the proposed DF-FD-VNLE with FD-LE and one iteration outperformed the FF-FD-VNLE in terms of the received SNR performance, while containing similar complexity. With the usage of FF-FD-VNLE before symbol decision, the nonlinearity-compensation performance of the DF-FD-VNLE can be further improved. Compared with conventional TD-VNLE, the RNRM of the one-iteration DF-FD-VNLE with FF-FD-VNLE (FD-LE) was reduced by a factor of as much as 82.19% (89.61%) at a memory length of 14 and a truncation factor of 3. Based on the one-iteration DF-FD-VNLE with FF-FD-VNLE, around 53.79 Gbit/s single wavelength OFDM IM-DD transmission over 60.8-km SSMF was successfully demonstrated at a BER of 3.8×10^{-3} and a ROP of -2 dBm, achieving 15% capacity improvement compared to the conventional TD-VNLE.

References

[1] White paper: Cisco VNI Forecast and Methodology, 2016.

[2] C. Y. Chuang, C. C. Wei, J. J. Liu, H. Y. Wu, H. M. Nguyen, C. W. Wang, S. Y. Li, Y. K. Chen, and J. Chen, "A high loss budget 400-Gbps WDM-OFDM long-reach PON over 60 km transmission by 10G-class EAM and PIN without in-line or pre-amplifier," *in Proc. Opt. Fiber Commun. Conf.*, Los Angeles, CA, USA, 2017, Paper W1K.3.

[3] ITUT G.989.1, "40-Gigabit-capable passive optical networks (NG-PON2): General requirements," 2013.

[4] K. Asaka and J. Kani, "Standardization trends for next-generation passive optical network stage 2 (NG-PON2)," *NTT Tech. Rev.*, vol. 13, no. 3, pp. 1–5, 2015.

[5] K. Zhong, X. Zhou, T. Gui, L. Tao, Y. Gao, W. Chen, J. Man, L. Zeng, A. P. T. Lau, and C. Lu, "Experimental study of PAM-4, CAP-16, and DMT for 100 Gb/s short reach optical transmission systems," *Opt. Express*, vol. 23, no. 2, pp. 1176–1189, Jan. 2015.

[6] K. Zhong, X. Zhou, J. Huo, C. Yu, C. Lu, and A. P. T. Lau, "Digital signal processing for short-reach optical communications: a review of current technologies and future trends," *J. Light. Technol.*, vol. 36, no. 2, pp. 377–400, Jan. 2018.

[7] N. Stojanovic, F. Karinou, Z. Qiang, and C. Prodaniuc, "Volterra and Wiener equalizers for short-reach 100G PAM-4 Applications," *J. Light. Technol.*, vol. 35, no. 21, pp. 4583–4594, Sep. 2017.

[8] H. Y. Chen, C.-C. Wei, I.-C. Lu, H.-H. Chu, Y.-C. Chen, and J. Chen, "High-Capacity and High-Loss-Budget OFDM Long-Reach PON Without an Optical Amplifier [Invited]," *J. Opt. Commun. Netw.*, vol. 7, no. 1, pp. A59–A65, Jan. 2015.

[9] H. Y. Chen, C. C. Wei, C. Y. Lin, L. W. Chen, I. C. Lu, and J. Chen, "Frequency-and time-domain nonlinear distortion compensation in high speed OFDM-IMDD LR-PON with high loss budget," *Opt. Express*, vol. 25, no. 5, pp. 5044–5056, Feb. 2017.

[10] J. Zhang, C. Guo, J. Liu, X. Wu, A. P. T. Lau, C. Lu, and S. Yu, "Low Complexity Frequency-Domain Nonlinear Equalization for 40-Gb/s/wavelength Long-Reach PON," *in Proc. Opt. Fiber Commun. Conf.*, San Diego, CA, USA, 2018, paper W1J.8.

[11] J. Zhang, Y. Zheng, X. Hong, and C. Guo, "Increase in Capacity of an IM/DD OFDM-PON Using Super-Nyquist Image Induced Aliasing and Simplified Nonlinear Equalization," *J. Light. Technol.*, vol. 35, no. 19, pp. 4105–4113, Aug. 2017.

[12] F. Nan, L. Nan, L. Chang, C. Xue, and P. Yand, "The High Power Budget IMDD OFDM-PON Down-stream Scheme Employing Sparse Volterra Filter-based Nonlinear Impairment Mitigation," *in CLEO*, San Jose, CA, USA, 2017, paper STh1O-1.

[13] J. Tsimbinos and K. V. Lever, "Computational complexity of Volterra based nonlinear compensators," *Electron. Lett.*, vol. 32, no. 9, pp. 852-854, Apr. 1996.

[14] M. Schetzen, "Theory of pth-order inverses of nonlinear systems," *IEEE Trans. Circuits Syst.*, vol. 23, no. 5, pp. 285–291, May 1976.

[15] A. Zaknich, Principles of adaptive filters and self-learning systems, *Springer Science & Business Media*, 2006.

[16] H. Sorensen, D. Jones, M. Heideman and C. Burrus, "Real-valued fast Fourier transform algorithms," *IEEE Trans. Acoust., Speech, Signal Process.*, vol. 35, no. 6, pp. 849–863, Jun. 1987.

[17] P. S. Chow, J. M. Cioffi, and J. A. C. Bingham, "A practical discrete multitone transceiver loading algorithm for data transmission over spectrally shaped channels," *IEEE Trans. Commun.*, vol. 43, no. 234, pp. 773–775, Aug. 1995.

[18] X. Liu, F. Buchali, "Intra-symbol frequency-domain averaging based channel estimation for coherent optical OFDM," *Opt. Express*, vol. 16, no. 26, pp. 21944–21957, Dec. 2008.